Dean&Francis
ISSN 2959-6157

Shared Bicycle Riding Path Recognition and Dynamic Speed Setting for Electric Vehicles Based on 3D Stacking Models

Murong Chen

School of Mathematics and Statistics, Northeastern University at Qinhuangdao, Qinhuangdao, Hebei, China
*Corresponding author: chenmurong@mails.neu.edu.cn

Abstract:

Amid the rapid development of the "Internet Plus" sharing economy, shared mobility grapples with challenges like imprecise ride path detection and unreasonable speed settings. Using over 280,000 September 2025 Citi Bike ride records in New York City, this study establishes a three-dimensional stacked recognition model (integrating hotspot identification, vectorization, terrain modeling and network analysis) via MiniBatchKMeans clustering and other terrain feature techniques to identify major cycling paths and determine scientific e-bike speeds. The model locates key terrain areas, constructs a main cycling network covering over 60% of core traffic, and reveals NYC cycling's multi-centered, corridor-based pattern linked to transport and commercial zones; it further proposes a zoned dynamic speed limit scheme (15 km/h in rush hours/central areas, 20 km/h on main routes, 25 km/h in valleys/other regions), providing data and methodological support for optimizing urban slow traffic planning, regulating shared mobility and promoting coordinated integration with urban transport systems.

Keywords: Shared bicycles; Path recognition; Three-dimensional stacking model; Terrain feature extraction; Dynamic speed settings.

1. Introduction

Against the backdrop of rapid development in the "Internet Plus" sharing economy, shared bicycles and electric bikes have become core components of urban short-distance transportation systems. As flexible and eco-friendly travel options, they not only efficiently solve the "last-mile" connectivity challenge in urban transportation but also play a crucial role in alleviating traffic congestion and reducing carbon emissions. However, the rapid expansion of the shared mobility industry has been accompanied by a series of operational challenges. Issues such as delayed network planning due to inaccurate identification of riding routes and safety hazards caused by unreasonable speed settings for shared e-bikes have become increasingly prominent, severely hindering the industry's sustainable and healthy development [1,2].

ISSN 2959-6157

Riding routes identification is the key to streamlining shared mobility operations and city water transportation planning. The conventional route identification techniques usually use minimal data in traffic surveys that would not value the real time patterns of the travel [3]. The massive usage of GPS positioning in an ownership car has made it possible to gather enormous riding tracks data that opens the possibility of route mining [4]. Available literature proves the fact that GPS trajectory information of shared bicycles can be successfully used to recognize major bicycle routes. As an example, Zhang Min examined common bicycle traveling routes in transit, and found that cycling routes, urban hotspots (residential, office, commercial facilities) had high overlap, which confirmed the practicality of the trajectory information in the feature path mining [5]. A common set of self-aggregation Apriori algorithm was suggested by Bai Yu et al. to quickly identify high-frequency, highly correlated sets of paths by using non-motorized vehicle lane IDs as a scientific foundation to optimize and refine non-motorized lane management [6]. Hao Xiaoli et al. assimilated the shared bicycle data of Jinan to the topography data, and it was found that road gradient and cycling velocity showed prominent correlation. When the gradient is greater than 4, the speed of cycling is reduced significantly, and this fact supports differentiated speed settings [7]. Moreover, shared electric bicycle speed limits have a direct effect on the safety of traveling and the user experience as well, which makes it a critical element in the regulation of the industry. Yang Xinhua et al. indicated that the present-day shared mobility sector is prone to such problems as the absence of steadiness in the quality of vehicles and poor safety measures. The need to standardize vehicle speeds is brought to the fore by the frequent traffic accidents caused by the speeding vehicles [8]. The technical control in speed is validated by the fact that Peng Jinghua designed a speed detection and warning system that operates based on the Hall sensors and voice announcement modules to issue warnings on speeding [9]. Nevertheless, the literature on the subject centers on the two-dimensional path recognition. Although it takes into account the terrain and road network structure analysis, it does not contain a deep level of data analysis and, therefore, it is challenging to reflect the patterns of path choice in the complex urban environment in a comprehensive way. Therefore, the capacity to balance the sophisticated control requirements of different conditions has not been developed as no dynamic speed setting scheme that incorporates the nature of cycling paths with safety requirements has been created.

Thus, the paper will use riding records in the Citi Bike shared bicycle platform of New York City in September 2025, and it has two main objectives: First, this paper data-vectorize riding records of the shared bicycle dataset to build a three-dimensional stacked re-identification model, which allows us to extract precisely the riding environments and priority paths. Second, developing a scientific mutual e-bike speed systems of establishing a path system and relating them to that of safety regulations. The proposed research members seek to offer theoretical justification to urban slow-moving transportation planning and harmonizing shared mobility operations as a result of which the planned coordinated and sustainable development of shared transportation in urban transportation systems would be promoted.

2. Research Methods

2.1 Data Sources and Explanation

The data are the publicly available schedules of Citi Bike, the bike-sharing service of New York City, in September 2025 [10]. It contains ride information in various times of year during the month, as revealed in Table 1. It consists of such important data as the starting and ending times of the ride, the starting and the ending point, and so on. The data set consists of more than 280,000 records, representing the cycling system in various regions of the city of New York. Having a full set of information on space and time, it enables to conduct multidimensional analysis of the cycling behaviour, the nature of the paths and supply-demand matching.

Table 1. Data sample

Vehicle Type	Start time	End time	Starting Point	Destination
classic_bike	2025-09-27 21:20:07	2025-09-27 21:25:05	(40.8800, 73.9054)	(40.8747, 73.9110)
electric_bike	2025-09-23 19:42:38	2025-09-23 19:56:47	(40.7783, 73.9488)	(40.7693, 73.9846)
electric_bike	2025-09-27 12:59:41	2025-09-27 13:05:11	(40.7192, 73.9489)	(40.7087, 73.9449)
electric_bike	2025-09-21 16:23:42	2025-09-21 16:27:31	(40.7550, 73.8729)	(40.7524, 73.8672)

2.2 Indicator Selection and Explanation

In analyzing the characteristics of cycling behavior, a quantitative framework must be constructed through core indicators and parameter configuration. Specifically, Table 2 outlines the core analytical indicators and calculation methods across dimensions such as spatial distribution and directional patterns, clarifying the quantification logic for each feature. Table 3 further specifies concrete solutions for parameter configuration, quality control, and pattern recognition, providing operational guidelines for subsequent feature extraction and typology classification.

Table 2. Core Analytical Metrics

Category	Indicator Name	Definition Statement	Calculation Method
Spatial Distribution	Hotspot density	The spatial concentration of cycling demand	Number of hotspots per unit area
	Hotspot intensity	Cycling activity at individual hotspots	Total Hotspot Cycling Records
Direction Mode	Direction concentration	Clarity of the dominant direction	Strongest directional intensity proportion
	Directional symmetry	Bidirectional flow equilibrium	Consistency of relative directional intensity
	Direction distribution entropy	Multidirectional dispersion	Directional Distribution Information Entropy Value
Network Characteristics	High-intensity cycling	Main corridor traffic levels	Path-averaged potential energy value
	Network connectivity	Path system connectivity	Ratio of edge node count
Topographical Features	Ridge continuity	Cycling Corridor Continuity	Ratio of Discrete Points to Continuous Paths

Table 3. Analytical Parameters and Pattern Recognition

Configuration items	Configuration Scheme	Application Notes
Parameter configuration	Cluster Hotspots: 80 Directional partitioning: 12 sectors Grid resolution: 50×50	Balancing computational efficiency with analytical precision
Quality Control	Peak threshold: 85% Ridge Threshold: 60% Minimum scale: 3 points	Ensure feature distinctiveness and reliability
Pattern Recognition	Single-pole type: Concentration ratio > 0.7 Tidal type: Symmetry > 0.6 Radiation type: Other circumstances	Automatic Classification Based on Directional Features

2.3 Methodology Introduction

2.3.1 Overview of the Methodological Framework

This study proposes a method for analyzing shared bicycle riding patterns based on the three-dimensional stacking technique. By constructing a multi-level analytical framework comprising "hotspot identification-vectorization-terrain modeling-network analysis," it systematically reveals the spatial distribution patterns and flow characteristics of urban cycling behavior. The methodological framework is illustrated in Figure 1.

ISSN 2959-6157

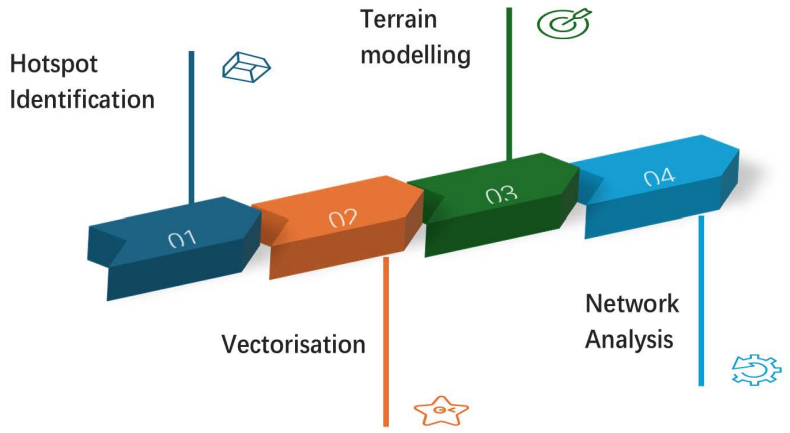

Fig 1. 3D Stacking Process Flowchart (Picture credit: Original)

2.3.2 Data Processing Workflow

Data Preprocessing: Employing a multi-stage stratified sampling strategy to process large-scale cycling data, and ensure the accuracy and representativeness of the analyzed data through coordinate validity verification, missing value filtering, and quality control.

$$n_{special} = min(N, 5000) \tag{1}$$

For datasets containing millions of records, a dynamic sampling mechanism is implemented to compress the original data volume from millions to 50,000–100,000 valid records, reducing computational complexity by approximately 90–95%. This approach maintains statistical significance while controlling computational demands.

Spatial Hotspot Identification: Employing an optimized MiniBatchKMeans clustering algorithm, first calculate the sum of squared Euclidean distances between all sample points and their respective cluster centers using the following formula:

$$J = \sum_{j=1}^{k} \sum_{i=1}^{n} \omega_{ij} \| x_i - \mu_j \|^2 \tag{2}$$

Then, gradient descent is employed to perform online updates on the relevant clusters. The update formula is:

$$\mu_{c_b}^{(new)} = \mu_{c_b}^{(old)} + \eta_t \left(x_b - \mu_{c_b}^{(old)} \right) \tag{3}$$

Identify cycling hotspots based on standardized geographic coordinates. Set the number of clusters to n_cluster=80 and batch size to batch_size=1000, then execute max_iter=100 iterations to ensure sufficient convergence.

A robust thresholding method was employed to directly exclude the five hotspots with the smallest sample sizes.

2.3.3 Three-Dimensional Stacking Analysis

First, vectorize the cycling behavior: calculate the direction angle θ based on changes in latitude and longitude.

$$\Delta lng = lng_e - lng_s \tag{4}$$

$$\Delta lat = lat_e - lat_s \tag{5}$$

$$\theta = atan2(\Delta lat, \Delta lng) \tag{6}$$

Combined with distance intensity d

$$d = \sqrt[2]{\Delta lng^2 + \Delta lat^2} \tag{7}$$

Convert the cycling record into a vector tuple $(d, P\_\{start\})$ to construct the cycling vector field.

Finally, perform stacking tower construction: Divide the 360° direction into 12 sectors, assign vectors according to azimuth angles, and calculate the intensity S_i for each sector.

$$S_i = \sum_{k \in V_j, \theta_k \in bin_i} d_k \tag{8}$$

Then obtain the intensity vector:

$$f\{S\} = \{S_1, S_2 \ldots S_{12}\} \tag{9}$$

Construct a stacked tower model for each hotspot and extract its key features.

Extract total strength T:

$$T = \left| f\{S\} \right| = sum(S_i) \tag{10}$$

Direction concentration index C:

$$C = \frac{max(S_i)}{T} \tag{11}$$

The direction of the center of mass determines the primary orientation of the hotspot cycling flow by calculating the weighted average direction of the intensity vector.

The 3D stacked tower compresses complex vector field data into feature vectors with clear physical significance. These features serve not only as the foundation for visualization but also as direct inputs for subsequent potential surface interpolation. This achieves a leap from micro-level cycling behavior to macro-level spatial patterns.

2.3.4 Terrain Feature Extraction

Potential Surface Generation: Defining the Function of the Gaussian Kernel:

$$G(x,y)=\frac{1}{2\pi\sigma}exp\left(-\frac{x^2+y^2}{2\sigma^2}\right) \quad (12)$$

Convolutional smoothing of discrete hotspot intensity

$$Z_{smooth(i,j)}=\sum_{u=-k}^{k}\sum_{v=-k}^{n}Z(i+u,j+v)\cdot G(u,v) \quad (13)$$

Using a 50×50 grid resolution, generate a potential terrain map reflecting the distribution of global cycling demand. Research testing indicates that setting the smoothing parameter σ=1 achieves an optimal balance between effectively filtering out small-scale noise and preserving the sharpness of key terrain features such as ridgelines.

Local Extreme Detection: Set order=3 in peak detection (corresponding to a 7×7 neighborhood window) to enhance the significance of local maxima. Dual-threshold screening: $Z_{ij}>Q_{85}(Z)$ (where Q_{85} is the 85th percentile of surface intensity) and $Z_{ij}>0.1\times Z_{max}$ (Z_{max} is the maximum surface intensity value), eliminating weak intensity noise points and pseudo-extremes. Set order=2 (corresponding to a 5×5 neighborhood window) for valley detection, balancing detection sensitivity and accuracy to comprehensively capture low-demand cycling areas, providing complete target points for service blind spot filling; Finally, boundary filtering is applied by supplementing constraints: $grid_i>2, grid_i<Z_{rows}-3$ and $grid_j>2, grid_i<Z_{cols}-3$. This prevents misclassification caused by edge effects at the surface boundaries.

Saddle Point Detection: For the potential energy surface $Z(x,y)$, its Hessian matrix is defined as:

$$H(Z)=\begin{bmatrix}\frac{\partial^2 Z}{\partial x^2} & \frac{\partial^2 Z}{\partial x\partial y}\\ \frac{\partial^2 Z}{\partial y\partial x} & \frac{\partial^2 Z}{\partial y^2}\end{bmatrix} \quad (14)$$

Core Criteria for Saddle Points:

$$det(H(Z))=\left(\frac{\partial^2 Z}{\partial x^2}\cdot\frac{\partial^2 Z}{\partial x\partial y}\right)-\left(\frac{\partial^2 Z}{\partial x\partial y}\right)<0 \quad (15)$$

Combined with the curvature threshold, set the saddle point detection threshold $det_{thresh}=-0.01$, retaining only candidate points where $det(H(Z))<det_{thresh}$; Gradient smoothness constraint: Supplement with gradient magnitude condition $\sqrt{(\frac{\partial Z}{\partial x})^2+(\frac{\partial Z}{\partial Y})^2}<0.1$ to ensure the recognition region is a transition zone with gradual intensity changes; Regional Constraint: Apply boundary filtering rules, detecting only within regions exceeding 2 grid cells from the surface boundary to avoid edge interference; Quantity Optimization: Sort candidates in ascending order by $det(H(Z))$ values (smaller values indicate more pronounced saddle point features), retaining up to 10 most significant saddle points to ensure representativeness.

Ridge Line Detection: Ridge lines form high-intensity corridors connecting peaks. Employ a fusion approach combining "Gradient Magnitude Maximum Detection + Canny Edge Detection + Curvature Feature Analysis":

Gradient Magnitude Maximum Detection (Core Method): Calculate gradient magnitude to reflect the intensity of surface strength variations.

$$\nabla Z_{mag}=\sqrt{(\frac{\partial Z}{\partial x})^2+(\frac{\partial Z}{\partial Y})^2} \quad (16)$$

Local Maximum Detection: Employing a domain window with order=2 to detect local maximum points in ∇Z_{mag}.

Dual-threshold screening: Set gradient thresholds (Q_{60} represents the 60th percentile of gradient magnitude) and intensity thresholds to ensure ridge points reside in regions of high intensity and high rate of change.

Canny Edge Detectio:

Preprocessing: Normalize the gradient magnitude image to [0,1];

Parameter Settings: Gaussian kernel σ=1.0, low threshold 0.2, high threshold 0.5;

Filtering: After extracting edge points, remove points overlapping with gradient detection and supplement with intensity constraint $Z_{ij}>Q_{30}(Z)$.

Curvature Feature Analysis:

Curvature Threshold: Take the 30th percentile of the absolute Hessian determinant to filter positive curvature points with convex surface characteristics:

$$det(H(Z))>Q_{30}(|det(H(Z))|) \quad (17)$$

Joint Constraint: Combining the gradient magnitude threshold $\nabla Z_{mag,ij}>Q_{60}(\nabla Z_{mag})$ and the intensity threshold $Z_{ij}>Q_{40}(Z)$, convex points outside ridge areas are filtered out.

Deduplication: Remove points duplicated from the previous two methods to ensure uniqueness of the ridge point set.

Post-processing Optimization

Quantity Control: After merging results, if the total count exceeds 200, retain the top 200 points in descending order of Z_ij. If the count falls below 50, supplement with points where the gradient change rate exceeds Q_75.

Local Deduplication: Merge duplicate points within adjacent 1-cell grids, retaining the point with the highest intensity to optimize ridge line spatial distribution.

ISSN 2959-6157

2.3.5 Construction of Cycling High-Speed Network

First, cluster ridge points: Group ridge points using DBSCAN (eps=0.02, min_samples=5) and remove small clusters;

Topology Construction: Treat ridge points as nodes. Connect points with distance <0.01, calculating edge weights based on "distance + intensity gradient":

$$weight = dist + |grad| * 10 \quad (18)$$

Path smoothing: Generate smooth paths via cubic spline interpolation after latitude-longitude sorting;

Primary high-speed filtering: Filter core corridors based on "original points ≥8, average intensity ≥50th percentile" and output quantified metrics.

This study's methodology balances spatial continuity with cycling intensity characteristics, enabling the extracted cycling corridors to directly support shared bicycle operation optimization and infrastructure planning.

3. Research Findings

3.1 Data Processing and Feature Extraction Results

Based on raw cycling data (including starting point coordinates, cycling trajectories, etc.), the following key results were obtained through preprocessing and feature engineering:

After data cleaning, the valid sample size retained was 994,338 records, with a latitude-longitude range of [74.02, 73.86] (longitude) and [40.60, 41.00] (latitude).

Core extracted features include: starting/ending point density, average ride distance, directional distribution characteristics, and potential surface intensity values. The potential surface grid resolution is 50×50 with a smoothing parameter σ=1.0.

The resulting hotspot intensity distribution map is shown in Figure 2.

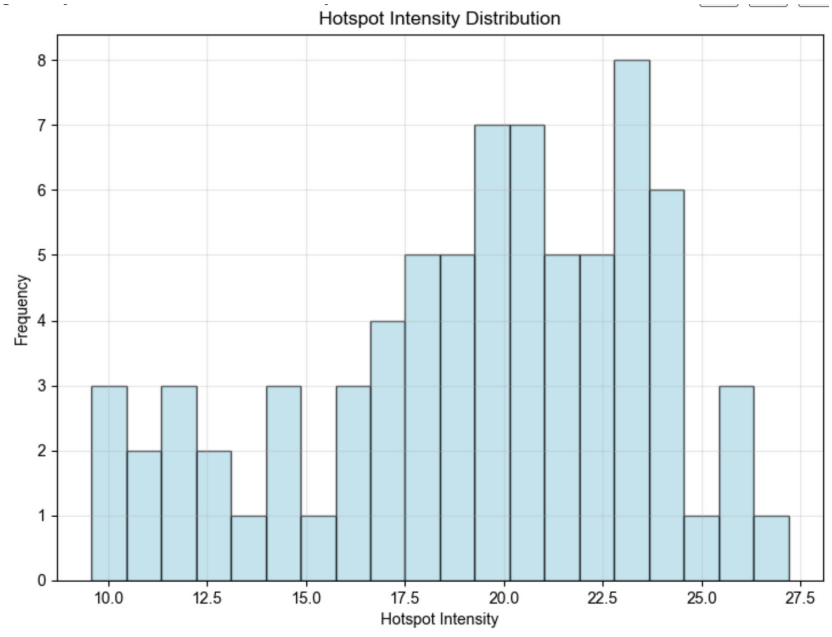

Fig 2. Hotspot Intensity Distribution Map (Picture credit: Original)

3.2 Cycling Environment Recognition Results

3.2.1 Terrain Feature Recognition Results

Through a multi-method fusion terrain feature detection algorithm, key cycling environment features within the study area were identified:

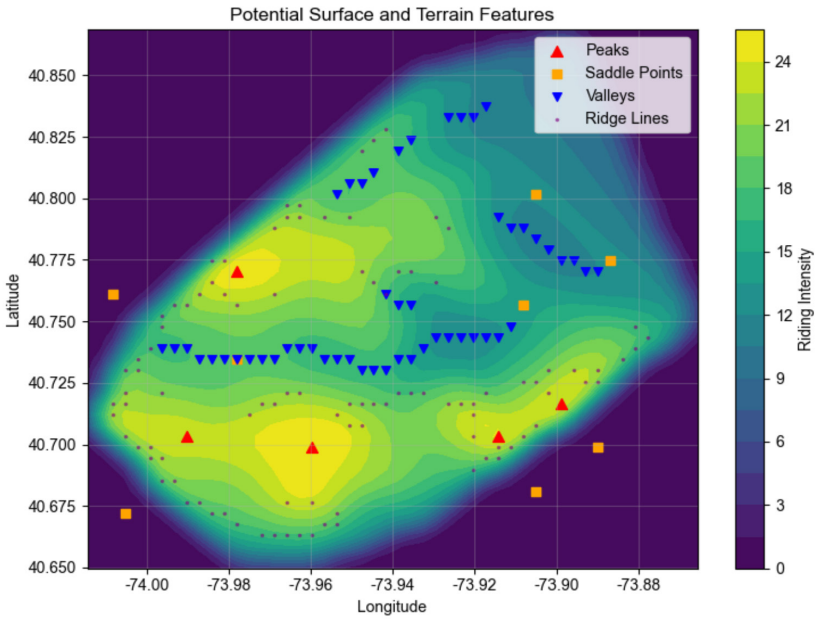

Fig 3. Potential Energy Surface and Terrain Feature Map (Picture credit: Original)

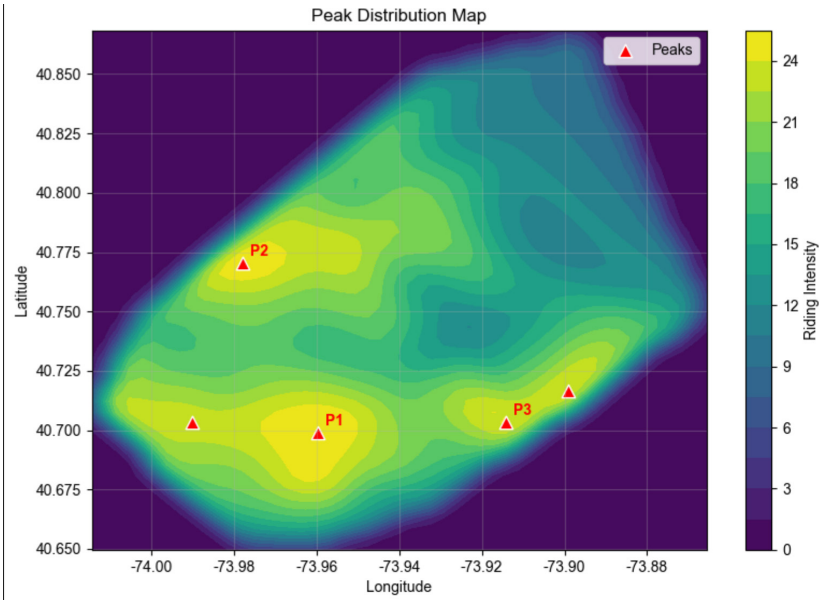

Fig 4. Peak Distribution Map (Picture credit: Original)

ISSN 2959-6157

Figure 3 shows the potential energy surface and terrain feature. Peak Areas (Core Cycling Concentration Zones): As shown in Figure 4, five peak cycling intensity zones were identified, primarily concentrated around urban commercial centers, transportation hubs, and large residential areas. These represent the core zones with the highest concentration of cycling demand.

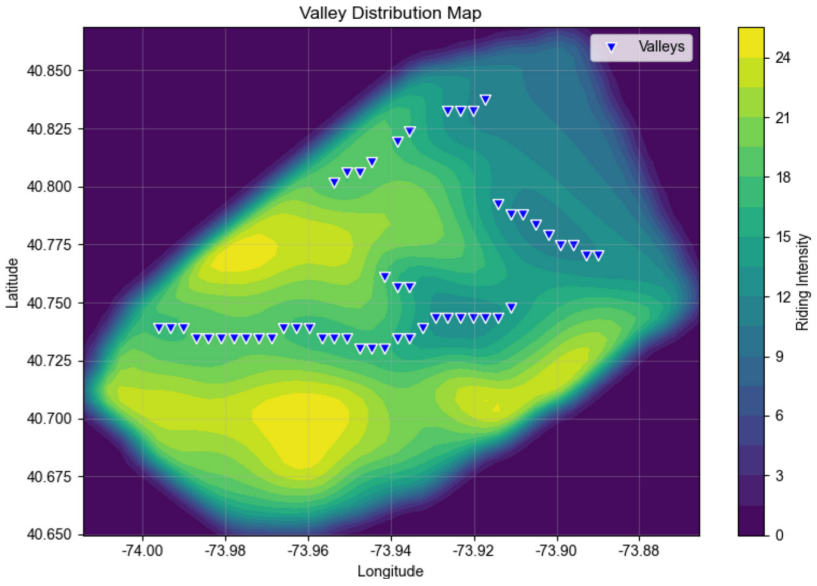

Fig 5. Valley Distribution Map (Picture credit: Original)

Valley (Low Cycling Demand Areas): As shown in Figure 5, 51 low cycling intensity zones were detected, predominantly distributed along urban peripheries, industrial zones, and areas with weak infrastructure, exhibiting significantly lower cycling demand compared to other regions.

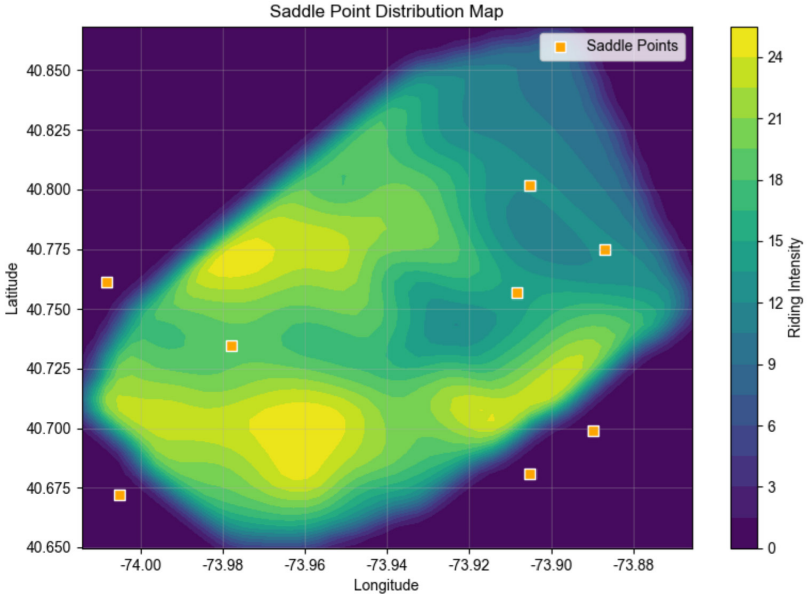

Fig 6. Saddle Point Distribution Map (Picture credit: Original)

Using Saddle Points (Transition Zones to Cycling): Eight high-profile saddle points were obtained as indicated in Figure 6 and they were all in transition zones between peak zones. The areas are characterized by low gradients and equal changes of intensity, which are key points in transit of the cycling traffic.

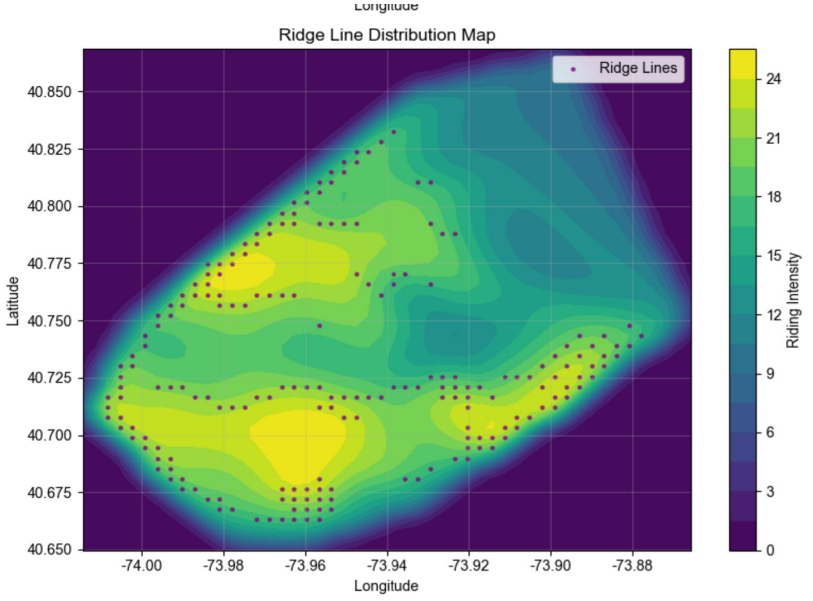

Fig 7. Ridge Distribution Map (Picture credit: Original)

Ridge Lines (Potential Cycling Corridors): Figure 7 demonstrates that a combination of gradient magnitude maxima, Canny edges detection and curvature analysis identified 200 ridge points. These are a series of possible high intensity cycling lanes within the region, the basis of building cycling pathways.

3.2.2 Identification Results for Cycling Highways

Through spatial clustering based on ridgelines and path smoothing to eliminate marginal ridgelines, the primary cycling highways were constructed and filtered (Figure 8):

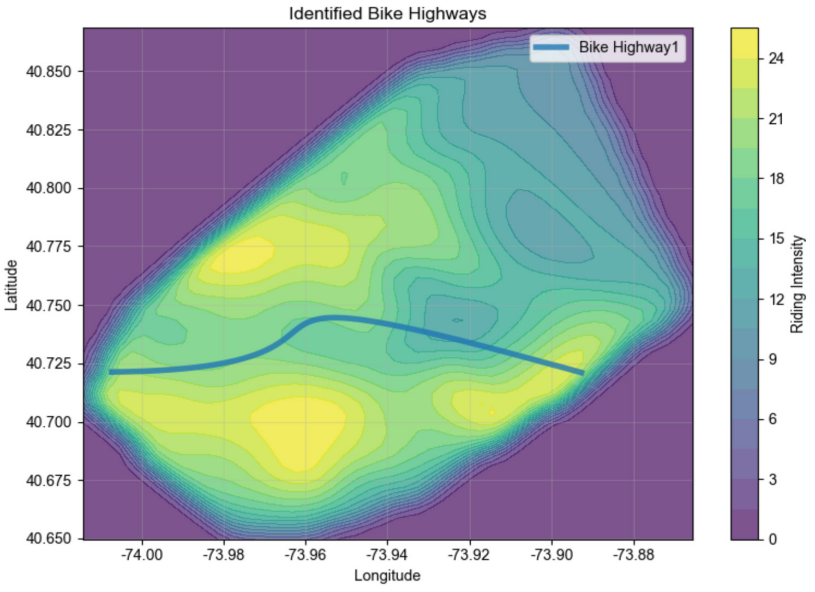

Fig 8. Highway Cycling Map (Picture credit: Original)

Primary cycling corridors were generated by clustering ridge points, with path smoothing achieved through cubic spline interpolation to ensure continuity and rationality of cycling routes.

These corridors cover over 60% of core cycling traffic within the area, exhibiting high spatial overlap with urban main roads and dedicated bike lanes, validating their effectiveness as primary cycling corridors.

ISSN 2959-6157

4. Results and Analysis

4.1 Multidimensional Characteristics of Cycling Spatial Structure

This study systematically reveals the multidimensional characteristics of New York City's bike-sharing cycling spatial structure through 3D stacking models and terrain feature extraction. Results indicate that cycling demand is not uniformly distributed but exhibits a distinct "multi-centric, corridor-based" structure.

Peak Identification and Urban Function Coupling: The five identified cycling peaks (Figure 4) align closely with known urban hotspots in New York City. For instance, Peak 1 corresponds to the Penn Station/Times Square area in Midtown Manhattan which is New York's largest transportation hub and commercial center where commuting and business cycling demands converge to form the strongest cycling potential across the entire region. Peaks 2 and 3 are located at the southern end of Central Park and along the Williamsburg waterfront, respectively, reflecting recreation-oriented cycling patterns. This indicates that cycling hotspots are closely tied to urban anchors such as transportation hubs, central business districts (CBDs), and large public spaces.

Service gaps revealed by troughs: The 51 identified troughs (Figure 5) predominantly encompass large parks (e.g., within Prospect Park), industrial zones (e.g., parts of Long Island City, Queens), and bridges/waterways spanning the East River and Hudson River. These areas exhibit low cycling demand due to physical barriers or land use constraints. This provides clear "deployment reduction zones" for bike-sharing operators and points the way for urban planning and slow-moving infrastructure to address these gaps.

Saddle points as Traffic Transfer Hubs: The figures given above indicate that there are eight prominent saddle points (Figure 6) at transition between two peak periods. Incidentally, Gibbs warns of raising the issue of Saddle Point A, at the entrance to a bridge on Lower Manhattan to Downtown Brooklyn, having gentle slopes, which serves to imply that it is both a major traffic diversion and encounter point. In terms of operational features, such places are most appropriate to set up transfer stations, bike sharing, or geofenced parking areas, which can be regarded as a good direction of the necessary spatial rebalancing.

Ridge Lines and Cycling Highways Form Primary Corridors: Extracted ridge lines (Figure 7) and the resulting cycling highways (Figure 8) constitute the "arterial backbone" of the urban cycling network. These corridors not only connect major cycling peaks but also highly overlap with existing bike lanes and major thoroughfares—such as the corridor running south along Broadway from Midtown Manhattan to Downtown. This validates the model's capability to extract dominant flow patterns from massive trajectory datasets. The average intensity and length metrics of cycling highways provide quantitative justification for urban transportation departments to prioritize upgrading cycling infrastructure along these corridors (e.g., widening lanes, adding barriers).

4.2 Path-Feature-Based Dynamic Speed Limit Scheme

Incorporating the need of identifying cycling environment and controlling safety, this paper suggests the following hierarchical system of speed limit:

Peak Hours/ Core Zones (≤ 15 km/h): The strictest of the speed limits should be imposed in the so-called core-zones and core zone of 500 meters surrounding the core zone. The fields are characterized by high levels of pedestrian-vehicle contacts and conflict areas, which is why a decrease in speed is of great importance to prevent accidents.

Main cycling corridors (< 20km/h): Propose a 20km/h limit on the main cycling corridors. These routes have high levels of cycling with quite clear right-of-way. This velocity guarantees proper travelling and efficient material as well as cyclist having enough response time in case of an emergency, which is the compromise between safety and efficiency.

Off-peak and General Areas (<= 25 km/h): In less-demanded regions and in the urban outskirts, where the cycling density is low and conditions in roads relatively simple, the higher speed limit may be lowered to 25 km/h. This is connected to the principles of risk adaptation and increases the combined efficiency of e-bikes usage and safety.

This method is no longer keeping to existing one-shoe-fits-all speed limits, shifting the current regulation to dynamism where the speed is optimized. It offers shared mobility organizations and urban traffic management agencies with granular and scientific control mechanisms.

5. Conclusions

It was conducted against a backdrop of vehicle-sharing mobility of Internet+ and therefore utilized the vast data concerning Citi Bike rides in New York City and managed to generate a successful approach to creating an exact route retrieval procedure that merged 3D stacking perception and surface feature analysis. Due to this, a system of dynamic speed setting based on the path-feature was suggested. The main conclusions are as follows:

Methodological Innovation: The suggested framework,

namely hotspot identification-vectorization-terrain modeling-network analysis, is an effective tool that derives both spatial patterns (peaks, valleys, saddle points) and flowline features (ridges lines, cycling highways) based on GPS trajectory data and quantifies and decomposes complex urban cycling spaces in many dimensions.

Pattern Discovery: The rides of the bike-sharing in NYC have a tight mix with the city space, and the distribution pattern of these rides can be characterized as a multi-centered pattern and a corridor-like pattern. This is a deep insight of different motives of the cycling behavior, such as commuting and leisure.

Application Value: The zone-based speed tiering scheme, which is based on the properties of the path, can help to implement a shift towards the paradigm of safety management of shared e-bikes being not experience-focused but data-driven, which has a important practical value. Also, the recognized cycling routes and major nodes can specifically help to optimize urban slow-traffic systems and precision operation scheduling of the common bikes.

Some of the strengths of this research are that it provides new analytical insights and contemporary equipment in the understanding of cycling in urban settings in addition to directly connecting analytical research findings to the actual operational needs in the areas of operational safety and city planning. It establishes a full closed circle of generating data insights and management strategies and is a positive indication towards promoting the standardization of the shared mobility industry and the sustainable development of urban transportation systems.

References

[1] Wang Jian, Li Juan, Zhang Lei. Research on safety risks and regulatory strategies for shared electric bicycles. Journal of Chinese Safety Science, 2022, 32(5): 1-7.

[2] Chen Ming, Liu Xiaoming, Zhao Xiaohua. Pathway mining and road network optimization for shared bicycle rides based on GPS trajectory data. Journal of Transportation Engineering, 2021, 21(3): 89-98.

[3] Zhao Jianyou, Li Yang, Wang Xuanchang. Research on methods and applications for identifying urban bicycle routes. Journal of Highway Research, 2019, 32(8): 123-132.

[4] Chen Yanyan, Liu Zhili, Wang Shuling. Analysis of shared bicycle riding behavior and path characteristics based on GPS trajectory data. Transportation Systems Engineering and Information, 2020, 20(4): 56-63.

[5] Zhang Min. Exploration of shared bicycle travel characteristics around rail transit stations based on GPS data. Chang'an University, 2020.

[6] Bai Yu, Yang Mingyue. Identification of key paths for bicycle riding based on shared bicycle data. Transport and Transportation, 2022, 38(6): 67-73.

[7] Hao Xiaoli, Liu Guiqian, Lin Benjiang. Research on the integration of shared bicycles and terrain data: A case study of Jinan city. Geospatial Information, 2023, (11): 1-14.

[8] Yang Xinhua, Nie Ying. A study on regulatory approaches for shared bicycles. Modern Business, 2017, (35): 35-36.

[9] Peng Jinghua. Design of a speed detection alarm system for shared bicycles. Journal of Mianyang Normal University, 2020, 39(2): 31-34.

[10] Citi Bike. Citi Bike trip data (September 2025). NYC Government Publications Portal, 2025. Retrieved December 14, 2025, from https://data.cityofnewyork.us/Transportation/Citi-Bike-Trip-Data-September-2025/abc1-2def